

REMOTE SENSING ANALYSIS OF ENVIRONMENTAL CHANGES IN A POST-MINING AREA: A CASE STUDY OF THE OLKUSZ REGION – PRELIMINARY RESULTS

Aleksandra SMENTEK¹, Jan BLACHOWSKI

¹Department of Geodesy and Geoinformatics, Faculty of Geoengineering, Mining and Geology,
Wrocław University of Science and Technology, Wrocław, Poland

Abstract

Continuous environmental monitoring of post-mining areas is essential, even years after the end of mining activity. Olkusz-Pomorzany mine closure in 2020 included shutting down the water pumps (2022), which resulted in the restoration of the underground water table and subsequent water appearing on the surface. The aim of this study is to analyse spatio-temporal water and vegetation changes in the post-mining and adjacent areas in Olkusz region, Poland, using remote sensing techniques on open-access satellite imagery data. The study uses nine Sentinel-2 images (2022-2024) and spectral indices (Modified Normalized Difference Water Index, Normalized Difference Vegetation Index) to identify and calculate the area of surface water and vegetation condition changes. Indices revealed a total water area of almost 400,000 m² and a substantial vegetation cover decrease. Using selected indices on open-access data allows the detection of surface water bodies and can provide preliminary results of spatio-temporal analysis of environmental changes in selected post-mining area.

Keywords: mining impacts, spectral indices, open-access satellite imagery, groundwater table restoration

1. INTRODUCTION

Mining activity affects the environment at all stages of operation, adversely interfering with land, soil, vegetation, air and water [1]. Ongoing mining activity is one aspect to be discussed in the concept of environmental hazards, another important one is the termination of mining activities and the process of mine closure, as well as the state of the environment in post-mining areas. Laurence (2006), lists many environmental risks of mine closure such as water, air and soil pollution due to acid mine drainage (AMD), land changes in infrastructure and flora and fauna, secondary ground movements, creation of dumps and tailing ponds, as well as social, legal and economic risks [2]. Sustainable mining practices

¹ Corresponding author: Aleksandra SMENTEK, Wrocław University of Science and Technology,
Faculty of Geoengineering, Mining and Geology, Na Grobli 15 st, 50-421 Wrocław, Poland, aleksandra.smentek@pwr.edu.pl

and environmental management are essential to maintain the well-being of the environment and therefore public safety.

One of the most common and dangerous impacts caused by underground mining are discontinuous ground movements such as sinkholes, as they can occur suddenly during mining operations, or years after the mining activity ends [3]. Despite that underground excavations are secured in the process of closing a mine, deformations can still occur. Mining related deformations occur due to the movement of overlying strata into the void caused by extraction of minerals and further due to mechanical suffosion and hydrological changes in the goaf. The location, size and extent of discontinuous deformation are mostly determined by the physical, geological and hydrological conditions of the earth, the depth and dimensions of the underground excavations, the method of mining and the liquidation of the goafs [4]. Mining activities very often require drainage of subsurface aquifers resulting in the development of depression cone due to mine dewatering, which causes hydrological drought [5]. Termination of such mines leads to restoration of the ground water table. The returning groundwater may naturally flood areas that subsided due to prior mining operation and create waterlogged areas or lakes from mine subsidence [6].

Continuous monitoring of the environment is an important step in controlling and minimizing the detrimental impact of mining activities. The use of satellite imagery and remote sensing techniques enables the efficient acquisition of information on a large area in a short time and study remote, difficult-to-access localizations safely. Satellite images are often available free of charge and stored in archives which makes them extremely useful for change analysis when there is no historical data. Moreover, images are acquired systematically, which allows multi-temporal analysis of the same area, and with the use of multispectral and hyperspectral satellite imagery it is possible to identify features imperceptible to the human eye [7].

Once mineral extraction is terminated, post-mining sites are rarely subjected to continuous or even periodic monitoring of environmental conditions due to high costs, lack of involvement after the mine closure, or ambiguity in responsibility e.g. due to a change of land ownership. Therefore, adverse effects emerging on the ground affecting the surface, landscape and infrastructure are often not monitored or mitigated.

Open data obtained by satellite systems provide means to effectively update information on post-mining area condition, e.g. Sentinel-1 acquires radar data for Satellite Radar Interferometry (InSAR) based monitoring of ground movements [8], [9], [10], whereas, Sentinel-2 provides multispectral imagery than can be used for calculation and analysis of spectral indices used as proxies for the assessment of vegetation condition [11], [12], [13]. Both sources can be used to detect water as demonstrated in [14], [15], [16].

Spectral indices are commonly used to identify various types of land cover. The most often used vegetation index is Normalized Difference Vegetation Index (NDVI). It is calculated from Red and Near Infra-Red (NIR) bands and as well as other vegetation indices, can be applied for analyses of mining and post-mining environment. [17] describes remote sensing of vegetation as useful in reclamation planning and further monitoring of the progress, identifying vegetated areas to determine their boundaries, and analyzing geological structures based on the vegetation condition. NDVI was used for example in [18] to analyze changes in the density of forest within mining area, in [19] to study multitemporal vegetation disturbance traits resulted from mining activities, in [20] to examine spatially uneven vegetation reaction to mining activities, [21] used NDVI to assess vegetation productivity in reclaimed areas of former coal and steel mines.

Other vegetation indices, along with the NDVI, were also used for the purpose of mining or post-mining environment monitoring. Indices such as Simple Ratio (SR), Reduced Simple Ratio (RSR), NDVI, Tasseled Cap Transformation were used in [22] to analyze multitemporal changes in vegetation

and monitor the reclamation progress of the open-pit coal mine, Ratio Vegetation Index (RVI), Enhanced Vegetation Index (EVI), and NDVI were used for a similar purpose in [23] to quantify vegetation changes over 15 years in a reclaimed coal mine. [24] used Normalized Difference Infrared Index (NDII), NDVI and Modified Triangular Vegetation Index (MTVI) to identify significant change of vegetation condition in time in the area of a former opencast and underground lignite mine.

For water identification, various water indices are used, as they differ in their performance characteristics. The Water Ratio Index (WRI) is used to estimate soil or vegetation water content [25], Sentinel-2 Water Index (SWI) utilizing Short Wave Infra-Red (SWIR) and, characteristic for Sentinel-2, Vegetation Red-Edge band can be applied to diverse land cover areas due to its proven superior performance in distinguishing urban areas, sediment, salt, and ice regions from water [26], [16]. Often, spectral indices are not directly used for identifying water bodies. Normalized Difference Water Index (NDWI), which is determined basing on Green and NIR bands, despite keyword “water” was proposed for remote measuring of liquid water molecules in vegetation canopies [27]. Modified Normalized Difference Water Index (MNDWI), however, is an enhanced version of NDWI, where NIR band is replaced by SWIR band, resulting in reduced noise from build-up areas, vegetation and soil [28].

Each post-mining area differs in characteristics of past mining operations, the process of mineral extraction system, land cover, type of geological structure, climate, type of occurring environmental hazard and its pace, timing, and impact on the environment, or reclamation activities done. This research focuses on analysing the environment in the post-mining Olkusz region (southern Poland).

In the past year, Olkusz region has been the centre of attention for the local community, media and the mine facility management due to environmental changes caused by impacts of recently concluded mining activity. Recent mine closure followed by shutting off the water pumps resulted in restoration of the underground water table and subsequent appearing of water on the surface, which resulted in the occurrence of subsidence lakes. The first signs of the formation of subsidence lakes were already noticed in early 2023 when, according to [29], the first surface water was observed. The formation of subsidence lakes is a progressive process over time, so it is necessary to conduct a multitemporal analysis.

Thus, this research aims to analyse spatio-temporal changes in surface water areas and vegetation condition in the post-mining Olkusz region, using remote sensing techniques applied to open-source multispectral satellite data. Additionally, it evaluates the chosen methodology. This approach enables multitemporal retrospective analyses, even in the absence of sufficient on-site measurements.

2. MATERIALS AND METHODS

2.1. Study area

The Olkusz region is located in Southern Poland, in Lesser Poland Voivodeship. The region known for zinc and lead ore deposits cover about 360 km² from Chechło in the north to the southern part of Olkusz and from Dąbrowa Górnicza in the west to the eastern part of Olkusz. This region encompasses the rivers Biała and Biała Przemsza (from southwest to the north), Sztola (southwest) and its tributary Baba (south). The local geological formations are characterised by alternating water-bearing and non-water-bearing formations. Four aquifers can be identified in: Quaternary, Jurassic, Triassic, and Palaeozoic formations. About 90% of the ore reserves are accumulated in the Triassic, mainly in ore-bearing dolomites, which is where a substantial amount of groundwater reserves is present. That complicated exploitation of the ore deposit. Mining activities had been conducted in this area for approximately ten centuries, with initial excavations from shallow deposits within Quaternary formations located above the water table or just below the water level. With advancements in technology, mining operations

expanded to greater depths, ranging from 70 to 190 meters [30]. Water inflows to the mine primarily originated from aquifers, with their volume increasing with mining depth; at a depth of 65 meters, inflows could reach approximately 40 m³/min, while at 140 meters, they may rise to around 270 m³/min. Precipitation insignificantly affects the size of the inflows only in extreme cases (such as flood) [31]. Figure 1a presents the location of the Olkusz region in Poland.

The mine's environmental impact was evident both during and after operations. Mining activities in the Olkusz area have led to significant landscape changes, a lowering of water table and subsequent hydrogeological drought, which have adversely affected the natural environment [5]. Waste material was stored in many small waste heaps containing large levels of cadmium, lead and zinc [32]. Water drained from the mine was discharged into rivers, with clean water being directed to the Baba River, and polluted water to the Biała River, where high nitrate content, and an increase in sulphate, calcium and magnesium were detected [30]. Additionally, discontinuous deformations have been occurring for years. Their cause was linked to the mining method without roof support used until the end of 1994 [29].

The termination of mining activities in the Olkusz region - closure of the last active mine Olkusz-Pomorzany in January 2021 and subsequent shutting of the water pumps (January 2022) impacted the environment in the area. The withheld supply of water from the mine to the rivers resulted in a partial dry-up and reduced flow in the rivers, which affected the surrounding environment [5]. The water flooding the mines may have impacted the underground geological structures and backfilled excavations, potentially leading to the rapid occurrence of discontinuous deformations in the area. The groundwater table has begun to restore, and water has appeared on the ground surface in the Olkusz area. Water flooded the subsidence areas, leading to the formation of subsidence lakes.

Based on [29] and visual analysis, two sites, within the Olkusz region, Hutki in the north and Bolesław in the south, where subsidence lakes occurred were selected as study areas (Fig. 1b). Figure 2 presents photography of a part of Bolesław subsidence lake taken in August 2024 [33].

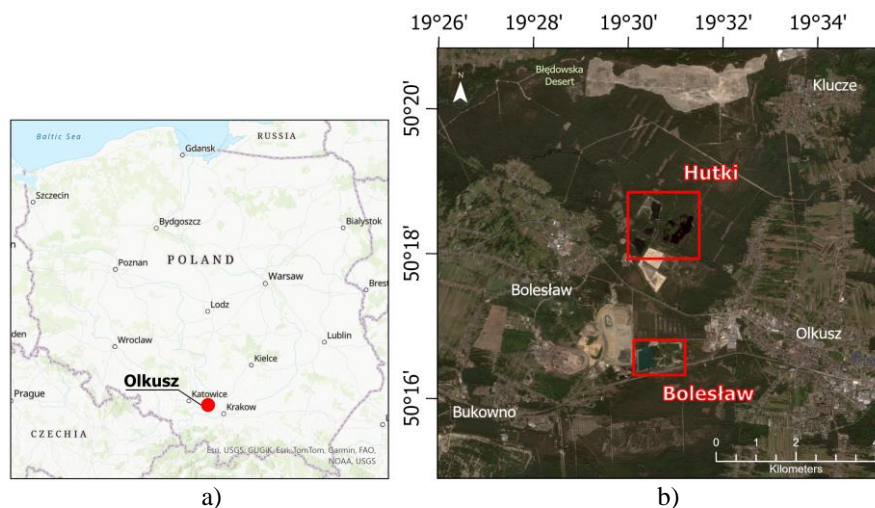


Fig. 1. a) Location of Olkusz region in Poland, b) Selected study areas in the Olkusz region



Fig. 2. Aerial view of subsidence lake that developed in the Bolesław post-mining area, August 2024 [33]

The Hutki study area covers 3,023,504 m² and is located in the northern part of Bolesław municipality. It is a region of the former backfilling sand open-pit mine “Hutki II” and historical mining of zinc. The area is mostly covered with vegetation, mainly tree canopy (mixed forests with a predominance of coniferous trees) [34].

The Bolesław area located south of Hutki and covers 1,153,234 m², it is a region of the Bolesław backfilling sand mine (‘current’ status mining area in 2019). Land cover consists of soil, sand (now covered by water), and vegetated areas, the majority of which are coniferous trees [34]. Figure 3 presents selected study areas. Boundaries were determined based on the latest satellite imagery of the subsidence lakes.

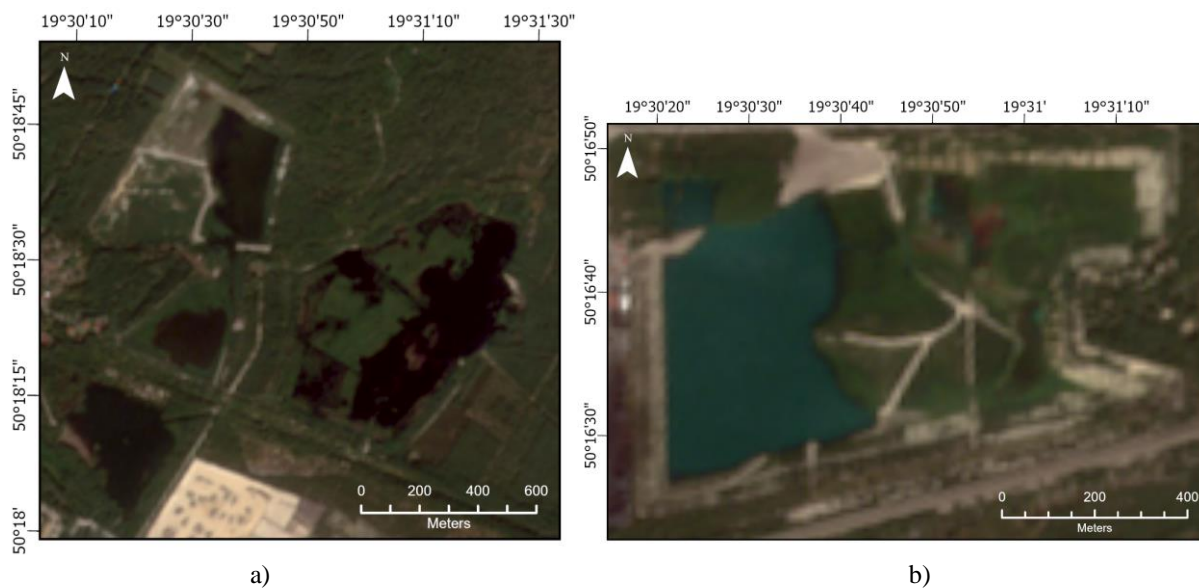


Fig. 3. Maps of the selected study areas: a) Hutki, b) Bolesław. (Sentinel-2 imagery, September 2024)

2.2. Data

This study uses multispectral satellite imagery data from open-source Sentinel-2 Level 2A Collection 1 archives. Sentinel-2 satellite provides free-of-charge images with a spatial resolution of 10, 20 or 60 meters, depending on the chosen spectral bands: 10 meters for Red, Green, Blue and NIR; 20 meters for SWIR and Vegetation Red-Edge; 60 meters for Coastal Aerosol, Water Vapour and SWIR Cirrus. Level 2A products are orthorectified and atmospherically corrected, which makes them ready to use right after downloading. The constellation of two polar-orbiting, sun-synchronous twin satellites Sentinel-2A and Sentinel-2B ensures a revisit time of 5 days. Every image is captured at 10:00 am (± 15 minutes) [35].

To analyse multitemporal changes in the chosen study areas, nine satellite images were acquired. The selection of data was based on its availability, minimal or no cloud coverage, and the timing of the phenomena's occurrence. According to [29], the water was first observed at the beginning of 2023. To study the area before the phenomenon occurred, the first image was acquired for August 2022. Subsequent analyses were carried out on images every 3 months, allowing for quarterly analysis and seasonal comparisons. Table 1 lists downloaded images and their details.

Table 1. Input imagery data specification

Image date	Year quarter	Image ID
27/08/2022	III	S2A_MSIL2A_20220827T093601_N0400_R036_T34UCA_20220827T142655
15/11/2022	IV	S2A_MSIL2A_20221115T094251_N0400_R036_T34UCA_20221115T141755
13/03/2023 *	I	S2B_MSIL2A_20230313T095039_N0509_R079_T34UCA_20230313T214900
03/06/2023	II	S2A_MSIL2A_20230603T094031_N0509_R036_T34UCA_20230603T135056
06/09/2023	III	S2B_MSIL2A_20230906T093549_N0509_R036_T34UCA_20230906T124337
28/12/2023 **	IV	S2B_MSIL2A_20231228T095329_N0510_R079_T34UCA_20231228T112733
29/03/2024	I	S2A_MSIL2A_20240329T094031_N0510_R036_T34UCA_20240329T125050
15/06/2024	II	S2B_MSIL2A_20240615T094549_N0510_R079_T34UCA_20240615T114834
05/09/2024	III	S2A_MSIL2A_20240905T094031_N0511_R036_T34UCA_20240905T133953

* - clouds

** - snow

Additionally, weather data on rainfall was acquired for the study of emerging water surfaces, helping to account for and exclude any potential impact on the results. The weather data was taken from the meteorological station at the AGH University of Science and Technology, located in Krakow (37 km from Bolesław and 40 km from Hutki), as it is the closest station providing open-source weather data [36]. The data was taken for the day prior to image capture and the day of imaging until 10:30 a.m. (time of satellite passage time). Precipitation occurred only on three days (Table 2), with no rainfall recorded on the remaining days. Due to the low sum of rainfall, it was considered that the detected water on the surface was not caused by precipitation.

Table 2. Precipitation data [36]

Date	Measured rainfall
12/03/2023	0.14 mm
27/12/2023	0.06 mm
28/03/2024	0.22 mm

2.3. Methodology

The chosen Sentinel-2 Level-2A atmospherically corrected products were pre-processed and prepared for further analyses. Pre-processing included resampling 20 m SWIR bands to 10 m rasters in order to use all available bands: band 4 - Red, band 3 - Green, band 2 - Blue, band 8 - NIR and band 11 - SWIR. Rasters were then clipped to study areas presented in Figure 3.

Considering the literature research discussed in the Introduction section and study area characteristics (waterbodies close to dense vegetation and soil areas) the following spectral indices were selected: Modified Normalized Difference Water Index (MNDWI) for water detection and the Normalized Difference Vegetation Index (NDVI) for vegetation condition analysis and water detection. These indices were calculated using equations 2.1 and 2.2 respectively [28], [37]. Threshold values were assigned based on the literature [38], [39], and characteristics of the study area. Indices values were then reclassified and renamed for further area calculations. Singular, scattered pixels indicated as water were considered as misclassified and excluded from the area calculations.

$$MNDWI = \frac{(GREEN - SWIR)}{(GREEN + SWIR)} \quad (2.1)$$

$$NDVI = \frac{(RED - NIR)}{(RED + NIR)} \quad (2.2)$$

To prevent possible errors resulting from indices marking clouds or snow as water, cloud and snow masks were applied. Only one image (13/03/2023, Hutki) required cloud masking, clouds covered less than 10% of the image therefore clouds were masked manually. Snow masking was also necessary for only a single image, captured on 20/12/2023, over both Hutki and Bolesław areas - the Normalized Difference Snow Index (NDSI) was used [40]. To address the potential overlap of snow cover on frozen water surfaces, which could affect the calculation of water surface area, NDSI raster was reclassified into 0 and 1 values and redefined using waterbody information derived from MNDWI raster from the next image (March 2024). Using image subtraction (NDSI raster - MNDWI raster) the redefined NDSI raster was obtained, where only snow-covered land areas were included, excluding snow-covered water areas. The selected indices' thresholds, reclassified values, and denotations are shown in Table 3.

Based on the indices' results, the surface water area was calculated for each image, and vegetation was analysed by examining changes in the healthy vegetation area. The results were analysed using descriptive statistics and statistical metrics including the calculation of the rate of increase. The methodology is depicted in Figure 4.

Table 3. Indices values and descriptions

Index	Index values	Value range description	Reclassified value	Reclassified description
MNDWI	-1.000 - 0.000	no water	0	excluded
	0.001 - 1.000	water	1	water
NDVI	-1.000 - 0.000	water	1	water
	0.001 - 0.100	bare ground, urban areas	2	no vegetation
	0.101 - 0.300	sparse/low condition vegetation	3	sparse vegetation
	0.301 - 0.500	moderate condition vegetation	4	healthy vegetation
0.501 - 1.000	good condition vegetation			
NDSI	-1.000 - 0.000	no snow	0	no snow
	0.001 - 1.000	snow	1	snow

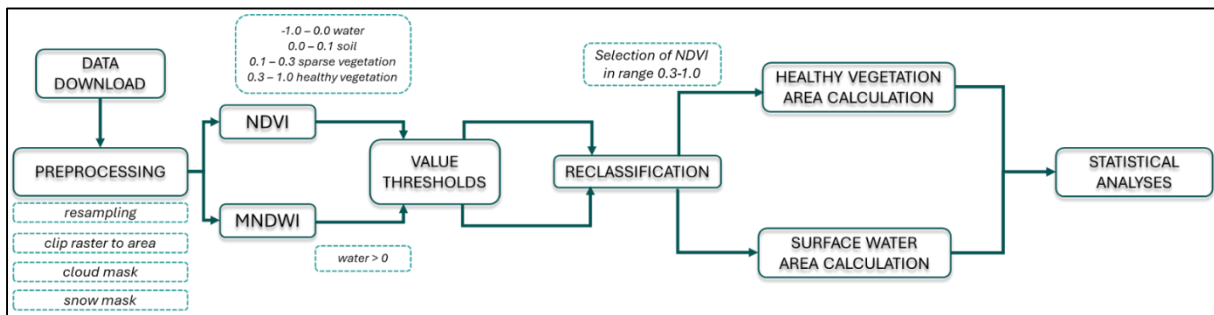


Fig. 4. Scheme of methodology

3. RESULTS AND DISCUSSION

As mentioned in the previous section, multi-temporal analysis in the Olkusz region was conducted on Sentinel-2 satellite imagery for the two-year period: 08/2022 - 09/2024. Analysis of spatio-temporal water and vegetation changes in the selected study areas “Bolesław” and “Hutki”, included calculating the areas of water bodies and healthy vegetation using the applied spectral indices: MNDWI for water detection and NDVI for vegetation and water analysis. Due to the lack of validation data (such as higher spatial resolution satellite imagery or in-situ measurements), the indices’ performance in the identification of water was assessed by visual analysis and comparison to the spectral images of the study areas. The results of the indices are layered on the satellite images displayed in the Colour Infra-Red (CIR) band composition for better perceptibility in visual analysis and comparison. CIR is a false-colour band composition consisting of NIR, Red, Green (instead of Red, Green, Blue). Displaying satellite images in CIR allows better discrimination of land cover types, especially between vegetation and water. In CIR composition, vegetation is represented by red (the more intense red colour the better vegetation condition) and water as dark, near-black regions [41].

Sections 3.1 and 3.2 include results and discussion for each study area. The results have been presented graphically as maps of the MNDWI index on the CIR composition and the results of the NDVI index for the nine dates from 27/08/2022 to 09/05/2024. The blue colour was used to mark the waterbody identified by the indices. The light and dark grey colours represent the mask of snow and clouds, respectively. Section 3.3. include statistical analyses for both regions.

3.1. Hutki area

Figure 5 shows the legend for NDVI maps. Figure 6 presents CIR composition maps with MNDWI, and NDVI maps in the Hutki area.

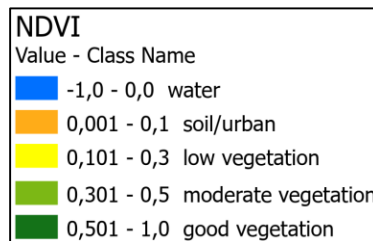
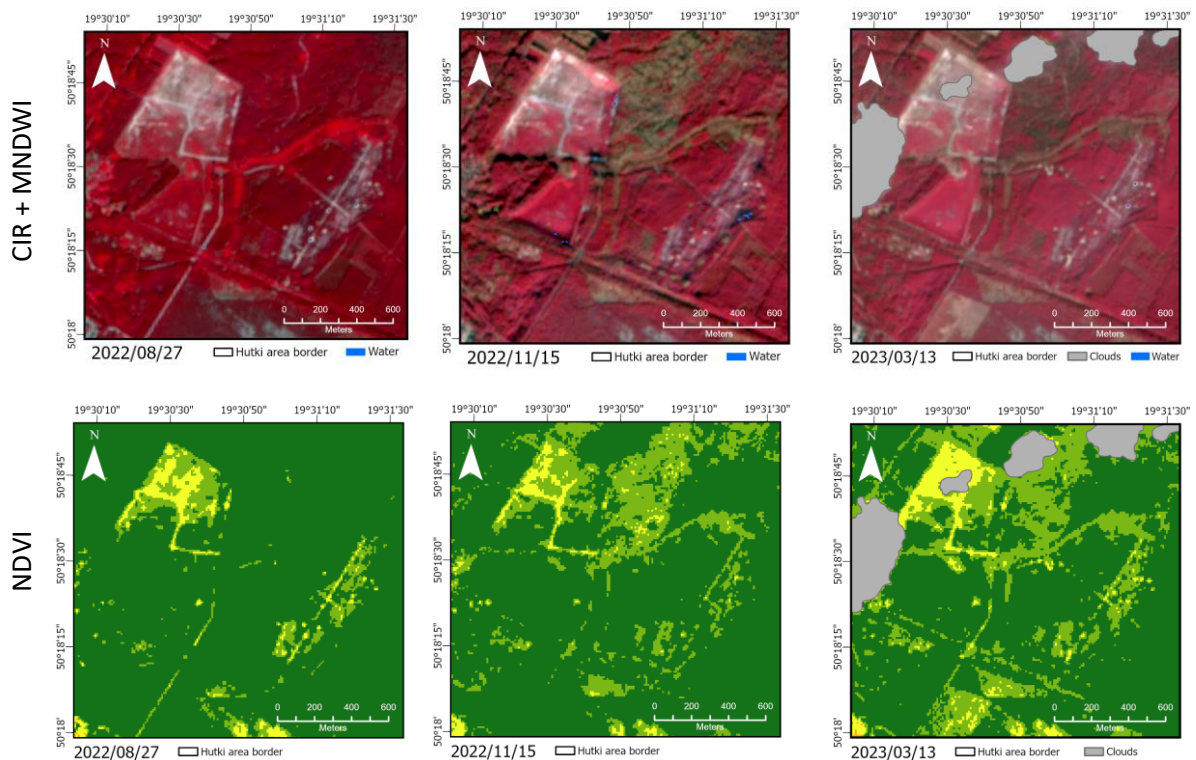


Fig. 5. NDVI legend



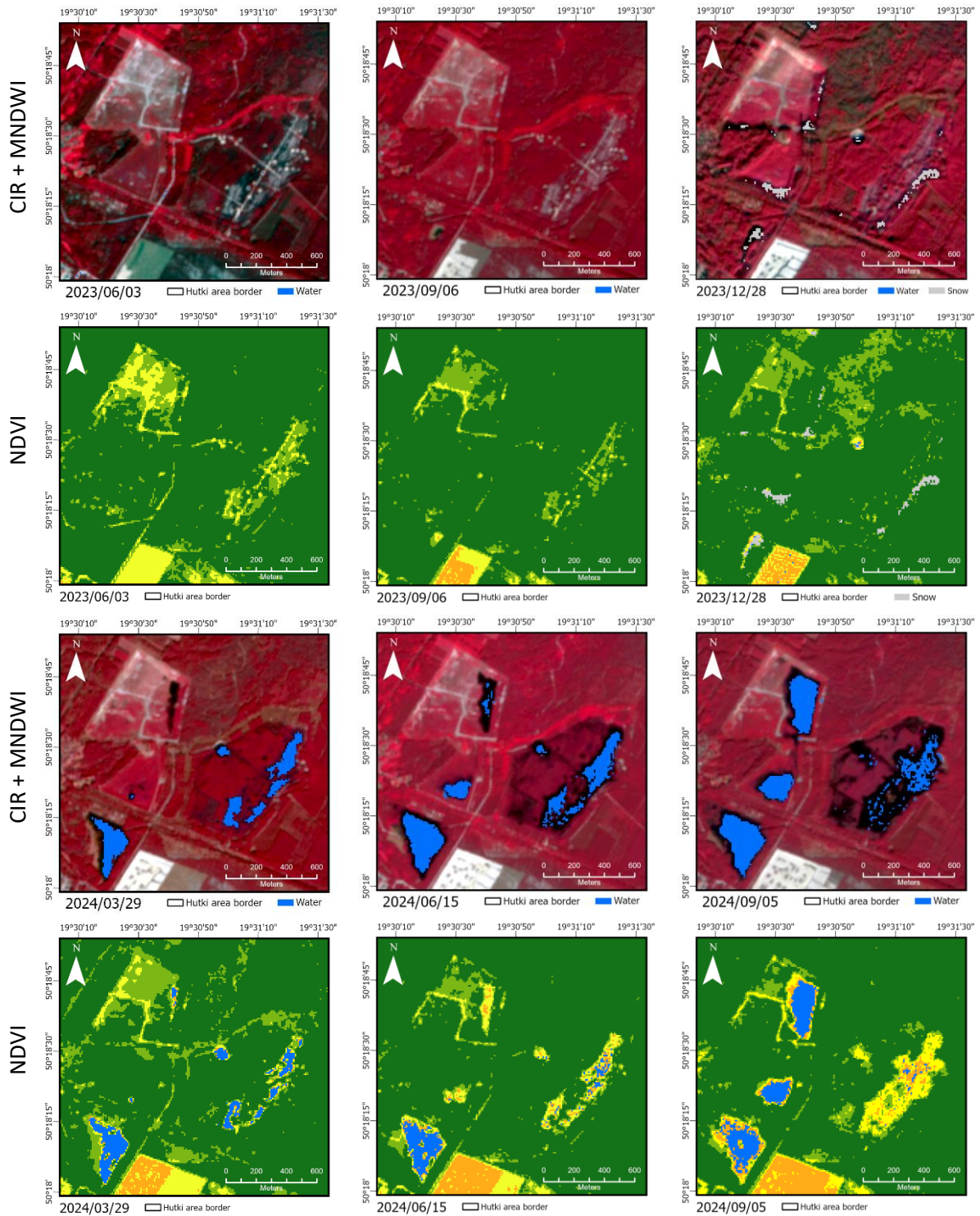


Fig. 6. CIR composition maps with MNDWI, and NDVI maps. Hutki area

Visual analysis of the results for the Hutki area indicates that the first waterlogged subsidence occurred in September 2023 in the southwestern part of the area. MNDWI and NDVI failed to identify the water, however, NDVI indicated deterioration of the vegetation condition in that area. Despite the increase in the lake area in December 2023, indices did not mark any pixels as water, until March 2024, when the water area expanded significantly, creating areas with subsidence lakes of varying shapes and sizes. In March 2024, MNDWI predominately correctly revealed waterlogged areas, with the exception of a lake with an elongated shape located in the northern part of the studied area. Moreover, few pixels were marked in round-shaped sinkhole of smaller area than the one in September 2023 (where water was not-indicated) and significantly smaller than the area of elongated lake. From March 2024 to September 2024, the surface area of these waterbodies increased significantly. The MNDWI delineates water mostly correctly, with minor deficiencies that are particularly evident in June 2024 in the northern and eastern parts of the area, and in September 2024 for the flooded parts in the eastern part, as well as along the edges of the subsidence lakes regardless of image date. NDVI is less effective than MNDWI in indicating water, and it tends to underestimate its extent. Vegetation index shows large area of vegetation deterioration in the southern part of the study area, visual comparison with RGB image indicates, that it has been transformed into a built-up area and therefore this change is considered unrelated to the formation of subsidence lakes. Comparing August 2022, September 2023 and September 2024 it is found that emerging water primarily caused the deterioration of healthy vegetation due to flooding. No significant adverse changes in vegetation are visible outside of the identified subsidence lakes. Moreover, a region of increasing healthy vegetation area was found in the north-west part of the area, in the vicinity of created subsidence lake. Vegetation condition also improved in the central-northern region of the Hutki area, NDVI revealed larger area of healthy vegetation in December 2023 and March 2024 compared to November 2022 and March 2023, respectively.

3.2. Bolesław area

Figure 7 shows the legend for NDVI maps. Figure 8 presents the CIR composition maps with MNDWI, and NDVI maps for the Bolesław study area.

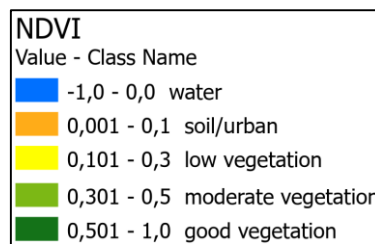
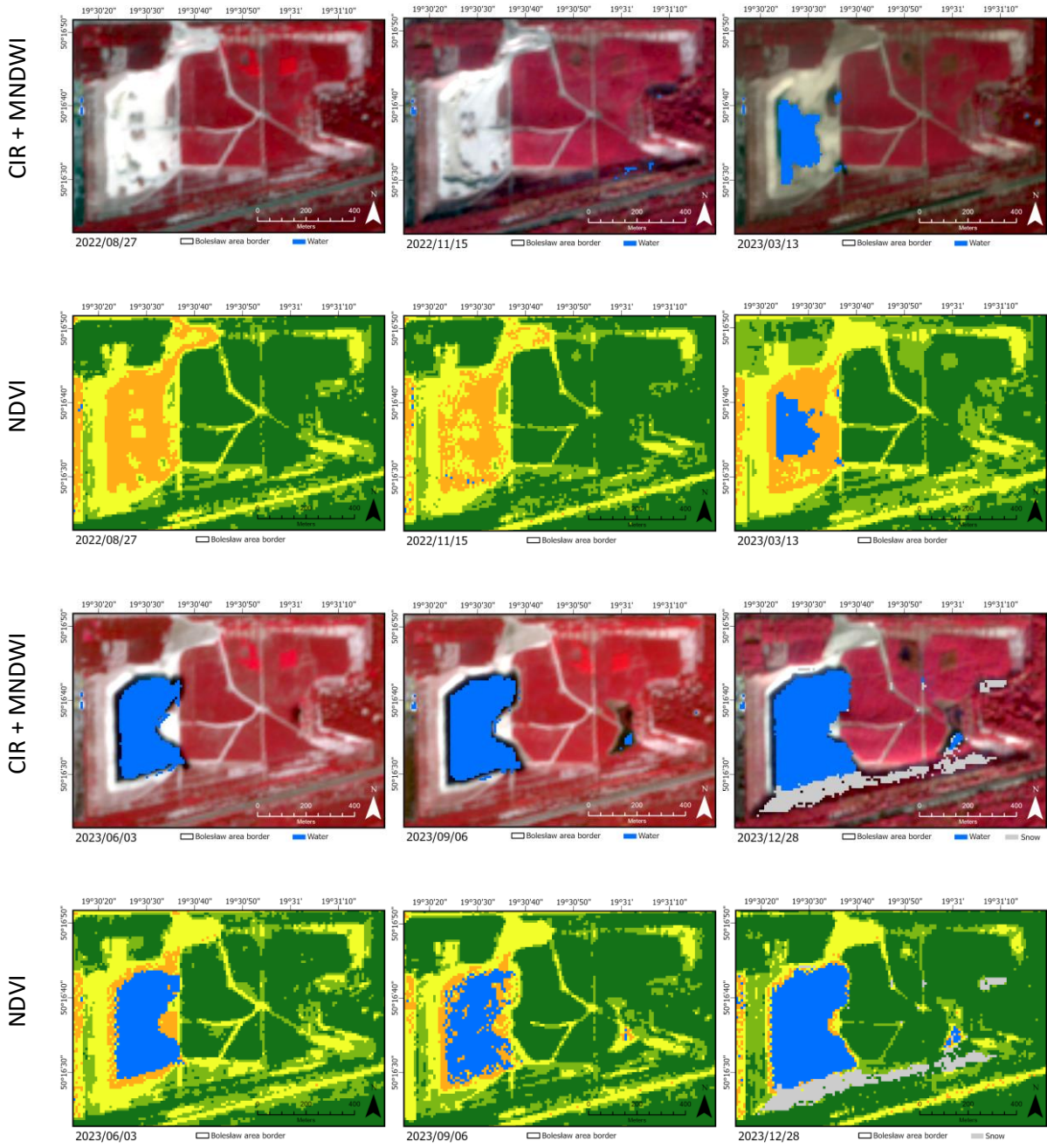


Fig. 7. NDVI legend



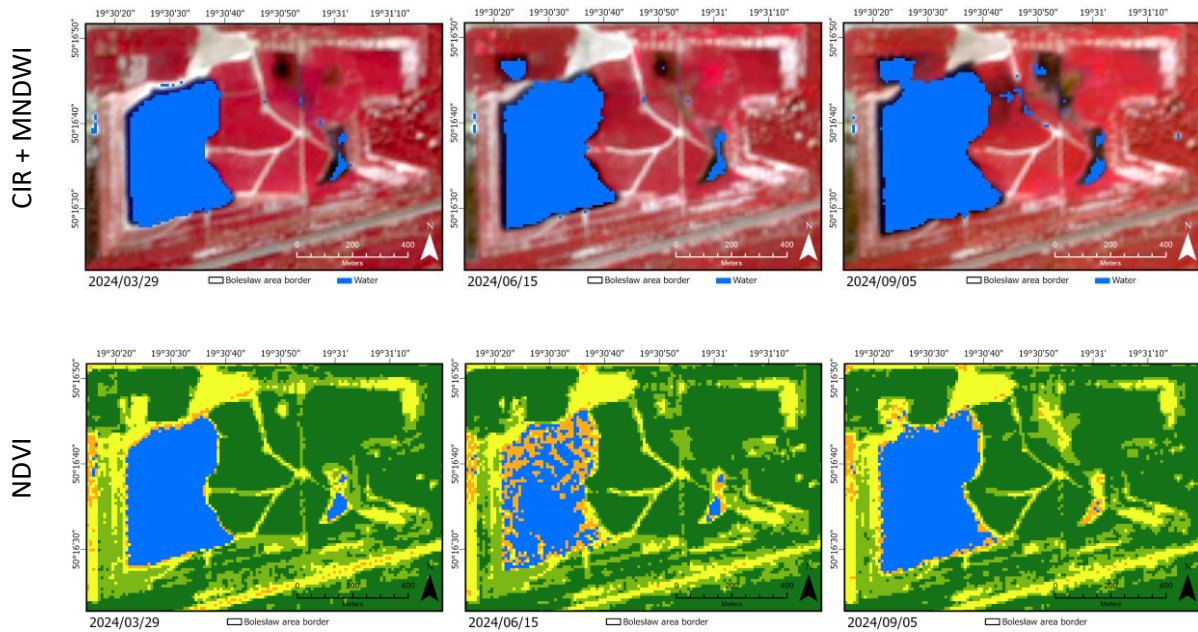


Fig. 8. CIR composition maps with MNDWI, and NDVI maps. Bolesław area

In the Bolesław study area water appeared earlier than in Hutki. In the data from March 2023 water had already covered a large part of the surface in the west part of the area. The MNDWI index identified one large waterbody and two smaller ones, which merged in June 2023 due to surface water area expansion. Visual analysis indicates a second subsidence lake that emerged on vegetated areas in the eastern part of the Area Of Interest (AOI) in June 2023. However, it was not evident in the MNDWI and NDVI results until September 2023. Similarly, waterlogged area in the central-north part, which appeared in December 2023, was not clearly identified by the water index, until September 2024, when only a few pixels were marked as water. The main, large subsidence lake has increased in area over time. It started to affect the surrounding vegetation extended from soil and sand areas to vegetated regions for the first time in June 2023. Therefore, the deterioration of the vegetation due to flood does not start immediately after the phenomena, contrary to Hutki region, and is less impacted by surface water. Furthermore, NDVI indicated improved condition of vegetation, which can be seen mainly in the western part of the area, along the lakes' border. MNDWI predominately correctly delineated water, with the errors in smaller, newly created lakes and at the border of the main waterlogged area. NDVI marked less water areas, however revealed severe adverse changes in vegetation condition in locations where MNDWI indicates water.

3.3. Statistical analysis

Based on applied spectral indices MNDWI and NDVI, areas of water and healthy vegetation were calculated. According to the established methodology, NDVI values ranging from 0.3 to 1.0 were considered to represent healthy vegetation. Figure 9 and Figure 10 present charts showing calculated surface water and healthy vegetation areas (square meters) in each analysed image since August 2022 to September 2024 in Hutki and Bolesław areas.

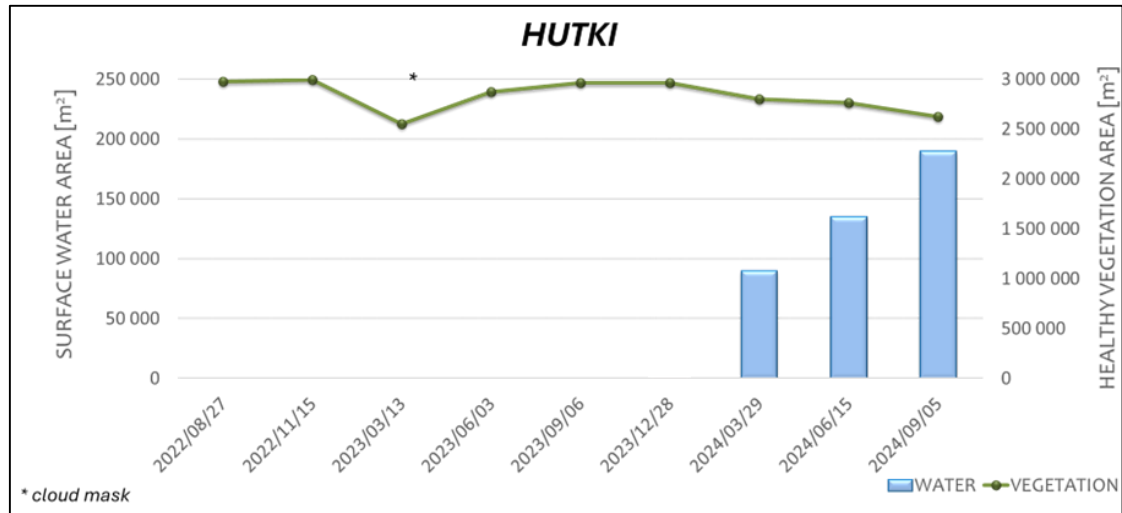


Fig. 9. Change of water and healthy vegetation areas between 27/08/2022 and 05/09/2024, Hutki study area

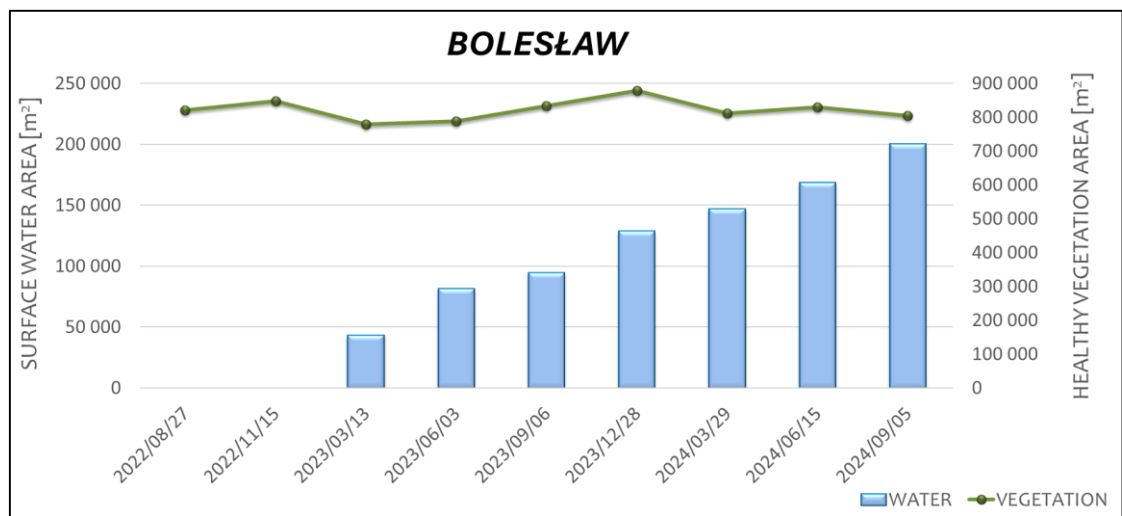


Fig. 10. Change of water and healthy vegetation areas between 27/08/2022 and 05/09/2024, Bolesław study area

In the Hutki site, MNDWI detected water in March 2024 when area reached 89,700 m². By September 2024, the identified water area increased to 189,000 m². Considering that in December 2023 no water was detected, the phenomena occurred rapidly. For the period from 12/2023 to 09/2024, the average water area increase rate is equal to 47,250 m² in 3 months. The sudden decrease in vegetation area measured in March 2023 is due to the applied cloud mask and, therefore, is not included in the analysis. Healthy vegetation area is almost constant before water appearance, only slightly decreased in June 2023 which correlates with development of built-up area. However, the later increase can indicate some improvement in vegetation condition. Decrease of healthy vegetation starting from December 2023 strongly coincides with the water appearance – therefore it can be assumed as the main cause of vegetation loss. In order to calculate the loss of the healthy vegetation area caused by emerging

surface water, the area of vegetation transformed into built-up (south part of Hutki site) was subtracted from the final calculations. Between 09/2023 and 09/2024 approximately 300,000 m² of healthy vegetation were lost (with additional 37,000 m² due to build-up development). Over 100,000 m² of healthy vegetation deteriorated indirectly due to creation of subsidence lakes.

In the Bolesław region MNDWI first identified water in March 2023, covering 43,000 m². Water area substantially increased reaching almost 200,000 m² in September 2024. When analysing the area every 3 months it was found that the water surface consistently and steadily increased, the increase rate between 11/2022 and 09/2024 is 25,000 m² in 3 months. As described in visual analysis of maps (Figure 8), healthy vegetation area is not directly and negatively impacted by the water occurrence due to water first appearing on non-vegetated area. Furthermore, healthy vegetation area increase and coincides with increase of the water area until December 2023. Decrease in healthy vegetation area from December 2024 correlates with the results of spectral indices and visual analysis findings of subsidence lakes exceeding or emerging on vegetated areas.

4. CONCLUSIONS

In this research, based on literature review, two water and vegetation spectral indices were applied on open-access satellite imagery data from Sentinel-2 to analyse spatio-temporal changes in the surface water area and in vegetation condition in the post-mining Olkusz region. The analysis was conducted in two selected study areas: Hutki and Bolesław.

The land condition was negatively affected by post-mining impacts, the mine drainage termination caused the water table to rise rapidly, which resulted in the appearance of water on the ground surface and creation of subsidence lakes.

Such phenomenon can be tracked back in time and effectively examined using remote sensing and satellite imagery. The chosen proxies for land cover condition based on NDVI and MNDWI indices applied on open-source Sentinel-2 images have been found useful in preliminary identification and analysis of surface water area and vegetation changes. The environmental changes can be quantified and summarized as follows, in September 2024, MNDWI based analysis indicated 189,000 m² of surface water in Hutki, and 200,000 m² in Bolesław. NDVI revealed 300,000 m² of deteriorated vegetation in Hutki area, and varying vegetation area in Bolesław. NDVI, despite being a vegetation index can also be applied to indicate water, however it under-estimates water compared to MNDWI. The latter index indicates waterbodies predominantly accurately, with lower accuracy on small waterbodies and areas where vegetation is mixed with water. In those areas NDVI indicates vegetation in poor condition – which can be used for detection of half-submerged vegetation areas.

Our results, with the selected indices acting as proxies for vegetation condition change and water occurrence, can only be considered as preliminary due to the data accuracy and quality. The accuracy of analysis is influenced by several factors such as spatial resolution of Sentinel-2 data (10-20 meters), characteristics of the study area that include zones with half-submerged vegetation and lack of in-situ data for validation. Future studies should include research on different spectral water indices or development of water index adjusted to study area characteristics, as well as validation analysis using for example higher spatial resolution data or field measurements. Moreover, due to rapid phenomena occurrence, higher temporal resolution will provide more detailed data on the progress of the phenomenon. More detailed multi-temporal analysis can be conducted using multi-source remotely sensed data such as Sentinel-1 for subsidence and water identification e.g. SAR Water Index (SWI), imagery from different satellite systems to improve temporal, spatial and spectral resolution, or airborne photogrammetric and laser scanning missions for high spatial resolution data and digital elevation models of the studied area.

REFERENCES

1. Jhariya, DC, Khan, R and Thakur, GS 2016. *Impact of Mining Activity on Water Resource: An Overview study*. Conference: National Seminar on Recent Practices & Innovations in Mining Industry (RPIMI 2016), Raipur, India, February 20216.
2. Laurence, D 2006. Optimisation of the mine closure process. *Journal of Cleaner Production* **14(3)**, 285–98.
3. Sanmiquel, L, Bascompta, M, Vintro, C and Yubero, T 2018. Subsidence Management System for Underground Mining. *Minerals* **8(6)**, 243.
4. Tajduś, K, Sroka, A, Misa, R and Dudek, M 2017. Przykłady zagrożeń powierzchni terenu deformacjami nieciągłymi typu powierzchniowego ujawniające się nad zlikwidowanymi podziemnymi wyrobiskami górnictwami [Examples of threats to the land surface by discontinuous deformations of the surface type revealed over decommissioned underground mine excavations]. *Prace Instytutu Mechaniki Górotworu PAN*, **19**, 3-10.
5. Lupa, M, Pełka, A, Młynarczyk, M, Staszal, J and Adamek, K 2023. Why Rivers Disappear—Remote Sensing Analysis of Postmining Factors Using the Example of the Sztoła River, Poland. *Remote Sensing*, **16(1)**, 111.
6. Mroczkowska, P and Biały, W 2015. Zwałowiska górnicze, a środowisko wodne na obszarach górniczych Republiki Czeskiej [Mining shafts, and the water environment in the mining areas of the Czech Republic]. *Systemy Wspomagania w Inżynierii Produkcji* (**3 (12)**), 132–41.
7. Sebnem Düzgün, H, Demirel, N 2011. *Remote Sensing of the Mine Environment*. London: CRC Press.
8. Gojković, Z, Kilibarda, M, Brajović, L, Marjanović, M, Milutinović, A and Ganić, A 2023. Ground Surface Subsidence Monitoring Using Sentinel-1 in the “Kostolac” Open Pit Coal Mine. *Remote Sensing* **15(10)**, 2519.
9. Pawłuszek-Filipiak, K, Wielgocka, N, Tondaś, D, Borkowski, A 2023. Monitoring nonlinear and fast deformation caused by underground mining exploitation using multi-temporal Sentinel-1 radar interferometry and corner reflectors: application, validation and processing obstacles. *International Journal of Digital Earth* **16(1)**, 251–271.
10. Declercq, PY, Dusar, M, Pirard, E, Verbeurgt, J, Choopani, A and Devleeschouwer, X 2023. Post Mining Ground Deformations Transition Related to Coal Mines Closure in the Campine Coal Basin, Belgium, Evidenced by Three Decades of MT-InSAR Data. *Remote Sensing* **15(3)**, 725.
11. Fabre, S, Elger, A, Riviere, T 2020. Exploitation of Sentinel-2 images for long-term vegetation monitoring at a former ore processing site, *Int. Arch. Photogramm. Remote Sens. Spatial Inf. Sci.*, **XLIII-B3-2020**, 1533–1537.
12. Orlov, S, Tsygulev, K, Sekrieru, R, Smagin, S and Smagin, A 2024. Remote Monitoring Algorithm for Vegetation Recovery on Mining Industry Sites. *Software Engineering Methods Design and Application*. Cham: Springer Nature Switzerland, p. 677–83.
13. Sun, X, Zhou, Y, Jia, S, Shao, H, Liu, M, Tao, S, Dai, X 2024. Impacts of mining on vegetation phenology and sensitivity assessment of spectral vegetation indices to mining activities in arid/semi-arid areas. *Journal of Environmental Management* **356**, 120678.
14. Saghafi, M, Ahmadi, A and Bigdeli, B 2021. Sentinel-1 and Sentinel-2 data fusion system for surface water extraction. *Journal of Applied Remote Sensing*, **Vol. 15, Issue 1**, 014521.
15. Bioresita, F, Puissant, A, Stumpf, A, Malet, JP 2019. Fusion of Sentinel-1 and Sentinel-2 image time series for permanent and temporary surface water mapping, *International Journal of Remote Sensing* **40:23**, 9026-9049.

16. Jiang, H, Wang, M, Hu, H, Xu, J 2021. Evaluating the Performance of Sentinel-1A and Sentinel-2 in Small Waterbody Mapping over Urban and Mountainous Regions. *Water*, **13**(7), 945.
17. Düzgün, H.S., & Demirel, N. 2011. Remote Sensing of the Mine Environment (1st ed.). London: CRC Press.
18. Nursaputra, M, et al, 2021. *The NDVI algorithm utilization on the google earth engine platform to monitor changes in forest density in mining area*, IOP Conf. Series: Earth and Environmental Science **886** (2021) 012100, 2nd Biennial Conference of Tropical Biodiversity, Makassar, Indonesia, 4 -5 August 2021.
19. Yang, Z, Shen, Y, Li, J, et al, 2022. Unsupervised monitoring of vegetation in a surface coal mining region based on NDVI time series. *Environmental Science and Pollution Research* **29**, 26539–26548.
20. Li, H, Xie, M, Wang, H, Li, S, Xu M 2020. Spatial Heterogeneity of Vegetation Response to Mining Activities in Resource Regions of Northwestern China. *Remote Sensing* **12**, no. 19, 3247.
21. Padmanaban, R, Bhowmik, AK, Cabral, P 2017. A Remote Sensing Approach to Environmental Monitoring in a Reclaimed Mine Area. *ISPRS International Journal of Geo-Information* **6**(12), 401.
22. Erner, A 2011. Remote sensing of vegetation health for reclaimed areas of Seyitömer open cast coal mine. *International Journal of Coal Geology* **V-86**(1), 20-26.
23. Karan, SK, Samadder, SR, Maiti, SK 2016. Assessment of the capability of remote sensing and GIS techniques for monitoring reclamation success in coal mine degraded lands. *Journal of Environmental Management* **V182**, 272-283.
24. Buczyńska, A, Blachowski, J, Bugajska-Jędraszek, N 2023. Analysis of Post-Mining Vegetation Development Using Remote Sensing and Spatial Regression Approach: A Case Study of Former Babina Mine (Western Poland). *Remote Sensing* **15**, 719.
25. Kareem, H H, Attaee, M H, Omran, Z A 2024. Estimation the Water Ratio Index (WRI) and Automated Water Extraction Index (AWEI) of Bath in The United Kingdom Using Remote Sensing Technology of The Multispectral Data of Landsat 8-Oli. *Water Conservation & Management* **8**(1), 171-178.
26. Jiang, W, Ni, Y, Pang, Z, He, G, Fu, J, Lu, J, Yang, K, Long, T, Lei, T 2020. A new index for identifying water body from Sentinel-2 satellite remote sensing imagery. *ISPRS Annals of the Photogrammetry, Remote Sensing and Spatial Information Sciences*, **V-3-2020**, 33-8.
27. Gao, B 1996. NDWI—A normalized difference water index for remote sensing of vegetation liquid water from space. *Remote Sensing of Environment* **58**(3), 257–66.
28. Xu, H 2006. Modification of normalised difference water index (NDWI) to enhance open water features in remotely sensed imagery. *International Journal of Remote Sensing* **27**(14), 3025–33.
29. ZGH Bolesław S.A. Likwidacja Kopalni. ZGH Bolesław, <https://zghboleslaw.pl/pl/aktualnosci/likwidacja-kopalni>. Accessed 20-11-2024
30. Niewdana, J, Świć, E 2011. *Żywioty w świecie podziemnych skarbów Olkuskich kopalń rud* [Elements in the world of underground treasures of Olkusz ore mines]. Bukowno: Zakłady Górniczo-Hutnicze BOLESŁAW S.A. w Bukownie.
31. Motyka, J, Adamczyk, Z, Juško, K 2016. Dopyływy wody do olkuskich kopalń rud cynku i ołowiu w ujęciu historycznym [Water inflows to Olkusz zinc and lead ore mines in historical perspective]. *Przegląd Górniczy* **Volume. 72, 6**, 49–58.
32. Woch, MW, Stefanowicz, AM, Stanek, M 2017. Waste heaps left by historical Zn-Pb ore mining are hotspots of species diversity of beech forest understory vegetation. *Science of The Total Environment* **599–600**, 32–41.

33. Photo by Rozmus, F, published by Olkusz.tv. Facebook, 17-08-2024. <https://www.facebook.com/Olkusz.tv>. Accessed 05-12-2024
34. Bureau for Forest Management and Geodesy - Forest Data Bank, <https://www.bdl.lasy.gov.pl/portal>, Accessed on 05-12-2024
35. European Space Agency. Sentinel-2. Copernicus Data Space Ecosystem, <https://dataspace.copernicus.eu/explore-data/data-collections/sentinel-data/sentinel-2>. Accessed 05-12-2024
36. AGH University of Science and Technology. Archival Weather Charts. AGH University, <http://meteo.ftj.agh.edu.pl/archivalCharts>. Accessed 05-12-2024
37. Kriegler, F J, Malila, W A, Nalepka, R F, Richardson, W 1969. *Preprocessing transformations and their effects on multispectral recognition*. Proceedings of the Sixth International Symposium on Remote Sensing of Environment, 97–131.
38. Huang, S, Tang, L, Hupy, JP, Wang, Y, Shao, G 2021. A commentary review on the use of normalized difference vegetation index (NDVI) in the era of popular remote sensing. *J For Res*, 32(1), 1–6.
39. Mehta, A, Shukla, S, Rakholia, S 2021. Vegetation Change Analysis using Normalized Difference Vegetation Index and Land Surface Temperature in Greater Gir Landscape. *Journal of Scientific Research* 65, 01–6.
40. Sentinel Hub. Normalized Difference Snow Index (NDSI). Sentinel Hub Custom Scripts, <https://custom-scripts.sentinel-hub.com/custom-scripts/sentinel-2/ndsi/>. Accessed 05-12-2024
41. EOS Data Analytics. Color Infrared (CIR) Imagery: Uses & Benefits. EOS, <https://eos.com/make-an-analysis/color-infrared/>. Accessed 05-12-2024